Article

Cell Reports

Differential Association of Chromatin Proteins Identifies BAF60a/SMARCD1 as a Regulator of Embryonic Stem Cell Differentiation

Graphical Abstract

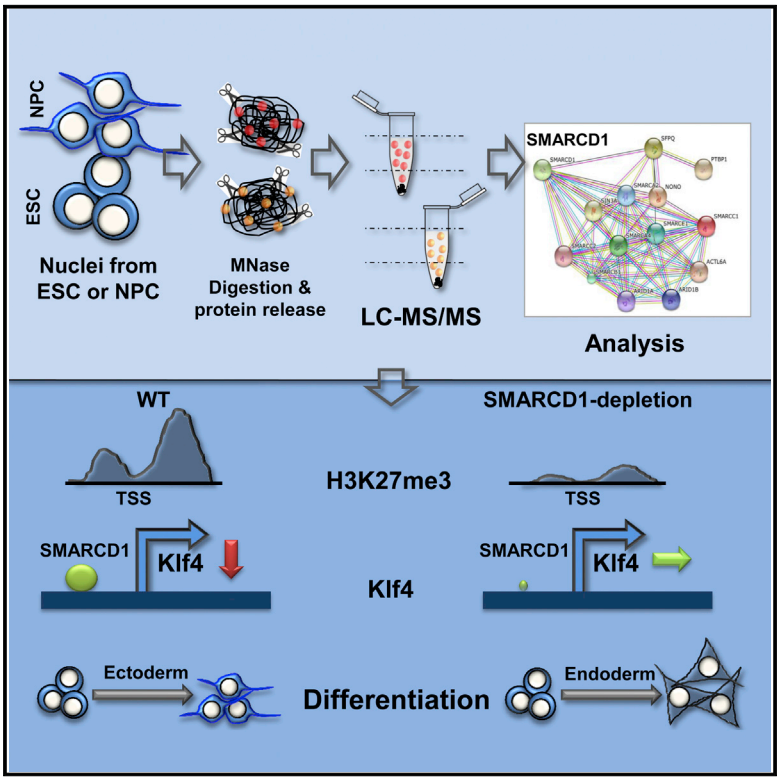

Authors

Adi Alajem, Alva Biran, ..., Siu Kwan Sze, Eran Meshorer

Correspondence

meshorer@huji.ac.il

In Brief

Alajem et al. develop an assay that indicates differential association of SMARCD1 with chromatin in embryonic stem cells (ESCs) and early-differentiating cells. SMARCD1 is associated with bivalent genes in ESCs, regulates H3K4me3/H3K27me3 distribution, and binds and regulates the pluripotency factor Klf4.

Highlights

- D-CAP identifies differentially bound chromatin proteins between different cell types
- SMARCD1, identified by D-CAP, regulates ectodermal differentiation of ESCs
- SMARCD1 is associated with bivalent genes and regulates H3K4me3/H3K27me3 distribution
- SMARCD1 binds and regulates Klf4 directly and indirectly

Accession Numbers

GSE65089

Alajem et al., 2015, Cell Reports *10*, 2019–2031
March 31, 2015
http://dx.doi.org/10.1016/j.celrep.2015.02.064

Cell Reports
Article

Differential Association of Chromatin Proteins Identifies BAF60a/SMARCD1 as a Regulator of Embryonic Stem Cell Differentiation

Adi Alajem,[1] Alva Biran,[1] Arigela Harikumar,[1] Badi Sri Sailaja,[1] Yair Aaronson,[1] Ilana Livyatan,[1] Malka Nissim-Rafinia,[1] Andreia Gianotti Sommer,[2] Gustavo Mostoslavsky,[2] Vincent R. Gerbasi,[3,4] Daniel E. Golden,[5] Arnab Datta,[6] Siu Kwan Sze,[6] and Eran Meshorer[1,7,*]

[1]Department of Genetics, Institute of Life Sciences, The Hebrew University of Jerusalem, Jerusalem 91904, Israel
[2]Section of Gastroenterology, Department of Medicine, Center for Regenerative Medicine (CReM), Boston University School of Medicine, 670 Albany Street, Suite 209, Boston, MA 02118, USA
[3]Department of Molecular Biosciences, Northwestern University, 2205 Tech Drive, Evanston, IL 60208, USA
[4]Naval Medical Research Center, Silver Spring, MD 20910, USA
[5]Merial Inc., a Sanofi Company, Duluth, GA 30096, USA
[6]School of Biological Sciences, Nanyang Technological University, 60 Nanyang Drive, Singapore 637551, Singapore
[7]The Edmond and Lily Safra Center for Brain Sciences, The Hebrew University of Jerusalem, Jerusalem 91904, Israel
*Correspondence: meshorer@huji.ac.il
http://dx.doi.org/10.1016/j.celrep.2015.02.064

SUMMARY

Embryonic stem cells (ESCs) possess a distinct chromatin conformation maintained by specialized chromatin proteins. To identify chromatin regulators in ESCs, we developed a simple biochemical assay named D-CAP (differential chromatin-associated proteins), using brief micrococcal nuclease digestion of chromatin, followed by liquid chromatography tandem mass spectrometry (LC-MS/MS). Using D-CAP, we identified several differentially chromatin-associated proteins between undifferentiated and differentiated ESCs, including the chromatin remodeling protein SMARCD1. SMARCD1 depletion in ESCs led to altered chromatin and enhanced endodermal differentiation. Gene expression and chromatin immunoprecipitation sequencing (ChIP-seq) analyses suggested that SMARCD1 is both an activator and a repressor and is enriched at developmental regulators and that its chromatin binding coincides with H3K27me3. SMARCD1 knockdown caused H3K27me3 redistribution and increased H3K4me3 around the transcription start site (TSS). One of the identified SMARCD1 targets was *Klf4*. In SMARCD1-knockdown clones, KLF4, as well as H3K4me3 at the *Klf4* locus, remained high and H3K27me3 was abolished. These results propose a role for SMARCD1 in restricting pluripotency and activating lineage pathways by regulating H3K27 methylation.

INTRODUCTION

Embryonic stem cells (ESCs) possess the remarkable ability to differentiate into any cell type of the three germ layers: endoderm, mesoderm, and ectoderm. This unique capacity is at least partially achieved owing to the distinct chromatin state of ESCs, described as more open (Gaspar-Maia et al., 2011), and their characteristic transcriptional network governed by OCT4, SOX2, and NANOG (Boyer et al., 2005; Chen et al., 2008; Skottman et al., 2005). Chromatin structure and function are maintained by histone modifications and chromatin remodeling proteins. Developmental genes in ESCs are bivalently marked by the "active" histone 3-lysine 4 trimethylation (H3K4me3) and the "repressive" H3K27me3. This allows developmental genes rapid activation or repression upon differentiation (Bernstein et al., 2006; Mikkelsen et al., 2007; Pan et al., 2007; Zhao et al., 2007).

Accumulating data suggest important roles for chromatin remodeling proteins in maintaining the characteristic chromatin state in ESCs (Gaspar-Maia et al., 2009; Lessard and Crabtree, 2010; Serrano et al., 2013). There are four different families of chromatin remodelers, each having a role in ESC biology: SWI/SNF (switch/sucrose non-fermentable), CHD (chromodomain helicase DNA binding), ISWI (imitation switch), and INO80 (inositol requiring 80 (Gaspar-Maia et al., 2011). The SWI/SNF family of chromatin remodelers has a special subunit composition in ESCs termed esBAF (BRG-associated factor) (Ho et al., 2009b). It was shown that several subunits of the esBAF complex (e.g., BRG1 and SMARCC1) are downregulated during differentiation (Efroni et al., 2008; Ho et al., 2009b), forming different complexes in differentiated cells (Ho et al., 2009b). BRG1 (a.k.a. SMARCA4), the catalytic subunit of esBAF, is essential for ESCs. BRG1 knockdown led to irregular ESC morphology, reduced proliferation rate, and decreased differentiation capacity (Efroni et al., 2008; Fazzio et al., 2008; Ho et al., 2009b; Kidder et al., 2009). Brg1 was found to support pluripotency by two opposing mechanisms: on one hand, enabling leukemia inhibitory factor (LIF) signaling by counteracting Polycomb group (PcG) proteins, and on the other hand, facilitating PcG function at its targets (Ho et al., 2011). In addition to Brg1, several other chromatin remodeling proteins were shown to regulate the

stem cell state (Gaspar-Maia et al., 2011; Lessard and Crabtree, 2010), suggesting a central role for chromatin remodelers in pluripotency maintenance and differentiation. Despite these recent advances, the molecular mechanisms and players that link chromatin, transcription, differentiation capacity, and pluripotency of stem cells have only been partially elucidated.

Here, we developed an unbiased approach for identifying chromatin-associated proteins that are specifically enriched on chromatin of pluripotent or differentiating ESCs but that can be applied to compare any two cell types, developmental stages, or various treatments. Unlike candidate-driven proteomics-based screens such as co-immunoprecipitation (co-IP), we analyzed all the released proteins in both cell states following micrococcal nuclease (MNase) digestion of chromatin, enabling us to identify cell-state-specific chromatin binding proteins by mass spectrometry. Using this approach, we identified SMARCD1 (a.k.a. BAF60a) as preferentially bound to chromatin in ESCs. SMARCD1 is a member of the SWI/SNF family and acts in recruiting transcription factors (TFs), such as Tbx1 and p53 (Chen et al., 2012; Oh et al., 2008), and nuclear receptors, such as the glucocorticoid receptor (Hsiao et al., 2003), to the SWI/SNF chromatin remodeling complex. The involvement of SMARCD1 in ESC biology was recently suggested by several studies. First, esBAF is enriched for SMARCD1 (Boyer et al., 2005; Ho et al., 2009b); second, genome-wide promoter analysis of DNA methylation in mouse ESCs and primary mouse embryonic fibroblasts (MEFs) showed that the *Smarcd1* promoter is hypomethylated in ESCs and hypermethylated in differentiated cells (Farthing et al., 2008); and third, a direct interaction between SMARCD1and SOX2 was identified in a recent proteomic study in ESCs (Gao et al., 2012).

In this work, we demonstrate the strength of our unbiased proteomic approach and specifically suggest a role for SMARCD1 in ESC biology. We show that SMARCD1-knockdown (SMARCD1-KD) ESCs exhibit altered chromatin and a perturbed differentiation phenotype. Gene expression analysis suggested that SMARCD1 acts as both an activator and a repressor. Chromatin immunoprecipitation (ChIP) followed by high-throughput sequencing (ChIP-seq) demonstrated that SMARCD1 is enriched in developmental regulators, that its binding pattern around transcription start sites (TSSs) is similar to that of H3K27me3, and that SMARCD1 depletion severely affects the global levels and distribution of H3K27me3. Taken together, these results suggest that SMARCD1 acts to restrict pluripotency and activate lineage programs during early commitment by regulating H3K27 methylation to facilitate differentiation.

RESULTS

Differential Association of Chromatin Proteins with Chromatin between Undifferentiated and Differentiated ESCs

In order to identify chromatin-associated proteins that are differentially associated with chromatin between different stages of differentiation, we developed an assay we named D-CAP (differential chromatin-associated proteins). In this assay, we purified nuclei from different stages of differentiation, thoroughly washed out all proteins that are not tightly associated with chromatin using consecutive low-salt buffer washes, and briefly treated with increasing levels of MNase. The brief MNase digestion releases chromatin-bound proteins, which are subsequently detected by liquid chromatography tandem mass spectrometry (LC-MS/MS) (Figure 1A). We performed D-CAP on purified nuclei from ESCs and from ESCs differentiated for 7 days along the neuronal lineage into neuronal progenitor cells (NPCs) (Efroni et al., 2008) (Figure S1). As might be expected from the more decondensed chromatin in undifferentiated ESCs, these cells displayed a slight preferential chromatin protein release, as we previously observed (Meshorer et al., 2006), but it should be noted that differential dynamics is not a general property of all chromatin proteins (Bošković et al., 2014; Meshorer et al., 2006) and thus reflects a unique biological feature of the differentially associated proteins.

Comparing mass spectrometry results between ESCs and NPCs identified chromatin-bound proteins characteristic of each state. An average of ~150 proteins were detected after mild treatment with MNase (3 or 4.5 U/ml), 49 of which were found exclusively in ESCs and 12 exclusively in NPCs (Table S1). Among the ESC-exclusive proteins, we identified SMARCC1 and SMARCD1 (a.k.a. BAF155 and BAF60a, respectively), both of which are chromatin remodeling proteins of the esBAF complex (Ho et al., 2009b).

To validate our analysis, we repeated the D-CAP assay and quantified the levels of SMARCC1 and SMARCD1 using western blots (WBs). Similar to the mass spectrometry results, we found that both proteins were released more readily in the undifferentiated state (Figure 1B). Additionally, to confirm this independently, we performed salt-extraction experiments where chromatin from ESCs and NPCs was subjected to increasing NaCl concentrations, and once again, SMARCC1 and SMARCD1 were released at lower salt concentrations in ESCs than in NPCs (Figure 1C). These results confirm that SMARCC1 and SMARCD1 are differentially associated with chromatin between ESCs and NPCs, as revealed by our D-CAP assay. Differential release was not due to differences in protein abundance between ESCs and NPCs, since the overall levels of both SMARCC1 and SMARCD1 did not change significantly (Figures 1B and 1C, input lanes).

SMARCD1 Depletion Has a Limited Effect in Undifferentiated ESCs

Several chromatin remodeling proteins have previously been identified to have important roles in ESC biology, including SMARCC1 (Ho et al., 2009b; Schaniel et al., 2009). We therefore focused our attention on another member of the esBAF complex, SMARCD1. To elucidate the role of SMARCD1 in ESCs, we generated both SMARCD1-knockout (SMARCD1-KO) clones using CRISPR/Cas9 (Figures S1D and S1E), as well as stable ESC lines constitutively expressing small hairpin RNAs (shRNAs) against SMARCD1 (Figures 2 and S2). SMARCD1 KO was tolerated in undifferentiated ESCs, but differentiation of these cells resulted in extensive cell death preventing careful examination of the SMARCD1-related phenotypes. We therefore concentrated on the SMARCD1-KD clones. SMARCD1 KD was verified in two separate clones (1a and 1b) and was found to be sustained at ~75% and ~50%, respectively, of SMARCD1 levels

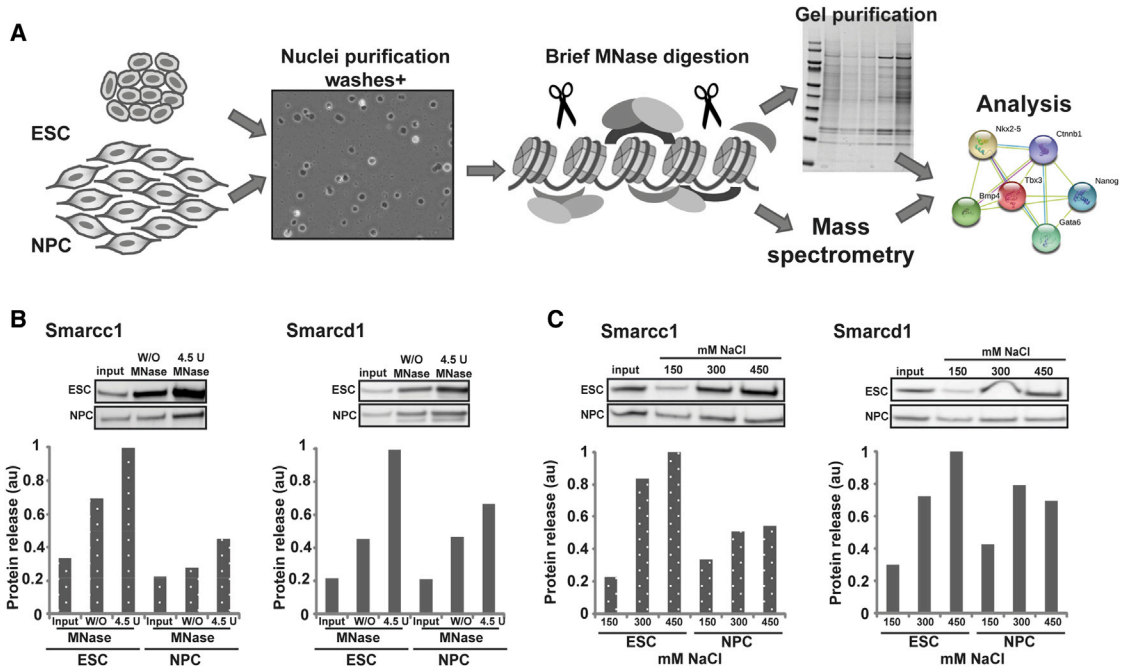

Figure 1. D-CAP Identifies SMARCD1 and SMARCC1 as Differentially Associated with Chromatin in ESCs Compared with NPCs

(A) A schematic description of the differential chromatin-associated proteins (D-CAP) method. Purified nuclei from both ESCs and NPCs are purified and washed four times with MNase digestion buffer. A brief MNase digestion is performed in order to release chromatin bound proteins. The released proteins can be subjected to gel purification or mass spectrometry analysis. Further analysis of the identified proteins can be performed using tools such as STRING.

(B) Western blot (WB) validation of the chromatin-association patterns of SMARCC1 and SMARCD1 using MNase. Input represents similar amounts of SMARCC1 (left) and SMARCD1 (right) in nuclei derived from ESCs and NPCs. "W/O MNase" represents the washed nuclear fraction incubated with the MNase buffer, without the MNase enzyme. "MNase" represents a 4.5 U/ml MNase treatment. Lanes 2 and 3 were treated similarly for 10 min at 37°C. Quantification is shown under each blot.

(C) Salt extraction of SMARCC1 and SMARCD1 using increasing amounts of NaCl. WB showing higher amounts of proteins released as a function of salt concentration. The graphs show WB quantification normalized to input. Input represents similar amounts of SMARCC1 (left) and SMARCD1 (right) in nuclei derived from ESCs and NPCs.

In (B) and (C), normalization of band intensity was done using ImageJ. Quantification is shown under each blot.

detected in a control line (S2) expressing scrambled oligo shRNA (Figures 2A and 2B) or in wild-type (WT) cells (not shown). SMARCD1-KD clones remained in their undifferentiated state; they formed compact colonies (Figure 2A), expressed the distinct ESC markers Oct4 and Nanog (Figures 2B and 2C), and maintained self-renewal properties and unaffected proliferation rates (Figure S2A). Additionally, SMARCD1-KD ESCs gave rise to teratomas showing indicative cell populations of all three germ layers (Figure S2B).

Since SMARCD1 is a chromatin remodeler, we examined whether KD of this protein affects chromatin protein dynamics and chromatin features as we have previously shown for the chromatin remodeling protein CHD1 (Gaspar-Maia et al., 2009). Fluorescence recovery after photobleaching (FRAP) analysis showed a significant change in the bleach depth of H1e-GFP upon knockdown (KD) of SMARCD1 (Figure S2C), indicating that the H1-GFP fraction in the KD cells is more mobile. In addition, using quantitative immunofluorescence, we tested marks of open chromatin and found that the levels of histone H3 acetylation (H3ac) were higher in the SMARCD1-KD clones (Figures 2D and 2E), although the levels of H3K4me3 were essentially unaltered between the SMARCD1-KD ESCs and the control cells (Figure S2D). We also tested the levels of two hallmarks of closed chromatin conformation including heterochromatin protein 1α (HP1α) and HP1γ, both of which remained unaltered in the undifferentiated state. HP1γ levels were determined by quantitative immunofluorescence (Figure 2C), and HP1α levels were quantified by western blots from chromatin fractions (Figure 2F). Although the expression level of HP1α did not change significantly in the undifferentiated state, its nuclear distribution was significantly altered, with a reduced number of heterochromatin foci per cell compared with controls (Figure 2G; $p < 0.05$, two-tailed Student's t test), opposite to what we previously observed in ESCs deficient for Chd1 (Gaspar-Maia et al., 2009). In retinoic acid (RA)-treated cells, HP1α was significantly reduced in the SMARCD1-KD clones (Figure 2F). The reduction of HP1α was confirmed in both the chromatin-bound and nucleoplasmic fractions to rule out differential distribution or chromatin association of HP1α. Taken together, these data demonstrate that while proliferation rate and pluripotency markers are overall unaffected in SMARCD1-KD cells, chromatin is globally more decondensed with reduced heterochromatin foci and somewhat elevated chromatin plasticity.

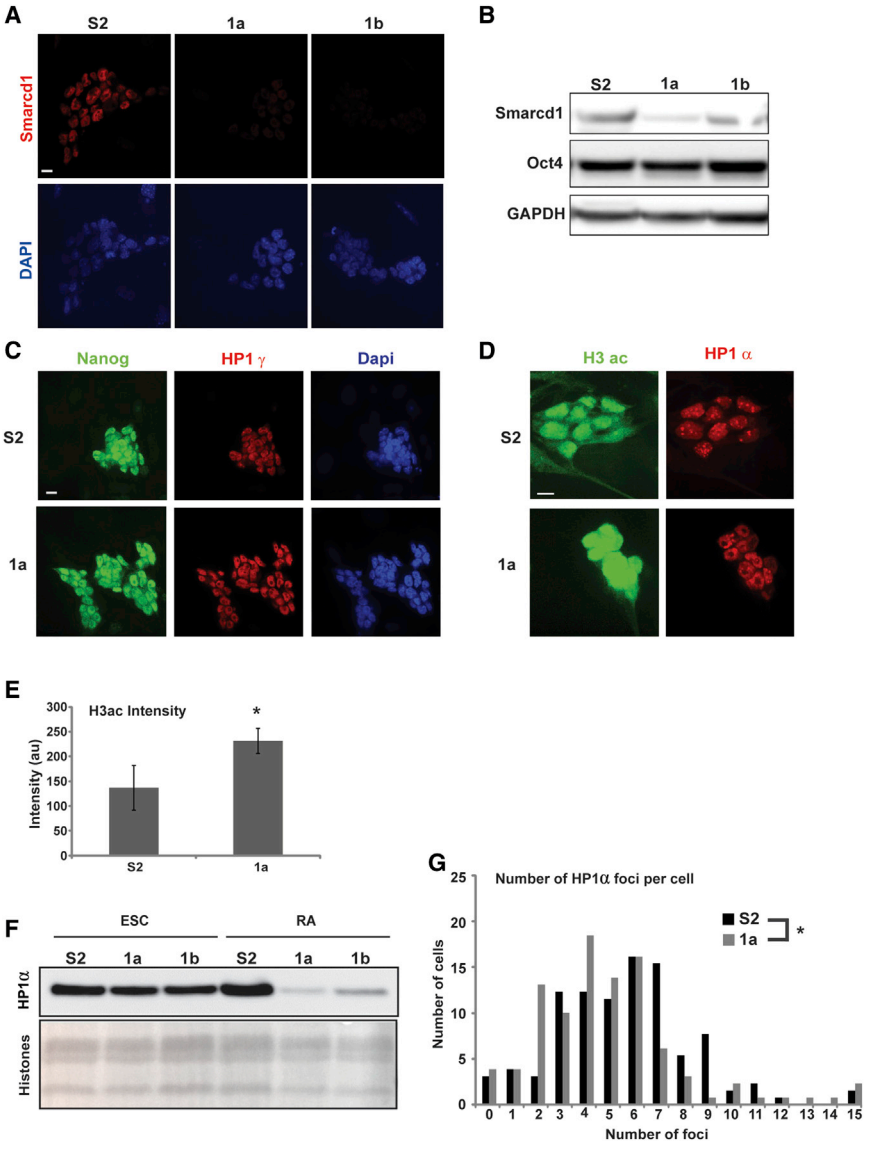

Figure 2. SMARCD1 Knockdown Affects Chromatin in ESCs and RA-Differentiated ESCs

(A) Immunostaining with anti-SMARCD1 antibodies (red, top) in SMARCD1-KD clones (1a and 1b) and in control cells (S2). Lower panel: DAPI.

(B) WB of SMARCD1 and OCT4 in SMARCD1-KD clones and controls (representative pictures from two independent experiments are shown). OCT4 levels did not change significantly.

(C) ESC-KD clones and controls were co-immunostained with anti-NANOG (green) and anti-HP1γ (red). Right panel: DAPI.

(D) ESC-KD clones and controls were co-immunostained with anti-H3ac (green) and anti-HP1α (red) showing high expression levels of H3ac and reduced number of HP1α foci in SMARCD1-KD cells.

(E) Quantification of H3ac fluorescence intensity. Changes are significant ($n = 110$; $p < 10^{-10}$, two-tailed Student's t test).

(F) WB showing HP1α levels in KD clones and controls in ESCs and in RA-differentiated ESCs (upper panel). Ponceau staining of core histones was used as a loading control (lower panel).

(G) Quantification of the number of HP1-positive heterochromatin foci in SMARCD1-KD versus controls. The average number of foci per nucleus was reduced from 5.6 in S2 to 4.9 in KD cells. Changes are significant ($n = 126$; $p < 0.05$, two-tailed Student's t test).

Scale bars in (A), (C), and (D) represent 10 μm.

SMARCD1 Is Necessary for Proper ESC Differentiation

As mentioned earlier, SMARCD1 KD did not alter Oct4 levels in undifferentiated ESCs and both SMARCD1-KO and SMARCD1-KD clones remained as undifferentiated ESCs when cultured on MEFs in the presence of LIF. To test the situation in differentiated cells, we subjected both cell types to embryoid body (EB) formation and examined the levels of OCT4 using WBs. We found that while in control cells OCT4 is dramatically reduced, as expected, the SMARCD1-KD clones failed to reduce OCT4 levels, which remained significantly higher than in control cells (Figure 3A). These data imply that SMARCD1 might have a role in silencing the pluripotency network upon differentiation. Supporting this notion, real-time quantitative RT-PCR (qPCR) for different markers demonstrated perturbed expression of an additional pluripotency factor, KLF4 (Figure 3B), which is also expressed during early endodermal differentiation (see below), as well as genes associated with ectoderm (Figure 3C), endoderm (Figure 3D) and mesoderm (Figures 3E and S3A) in differentiating SMARCD1-KD EBs.

We next tested the effects of SMARCD1 reduction on differentiation into specific lineages, including mesoderm (cardiomyocytes) and ectoderm (NPCs and RA-induced differentiation). In the initial stages of mesodermal differentiation, the morphology of EB formation as well as re-plating, monolayer spreading, and cell proliferation was seemingly unaffected, but at differentiation day 10, KD clones showed a remarkable 10-fold reduction in the number of beating foci compared to control cells (Figure 4A). Real-time qPCR analysis for cardiomyocyte markers at differentiation day 12 showed a significant reduction (ranging from 3- to 33-fold) in the expression levels of the three mesodermal markers tested, including Alcam, Tnnt2, and Nppa (Figure 4B). The early stages of ectodermal differentiation were also unaffected, with KD cells properly forming EBs, although when these EBs were re-plated in NPC-inducing medium, they gave rise to 4-fold fewer NPCs compared to control cells (Figures 4C and 4D). In RA-induced differentiating cells, which remain as a monolayer and do not transition through an EB stage, SMARCD1 reduction notably altered cell morphology, with shrunk cytoplasms compared with control cells, and a 40% reduction in cell length (Figures 4E and 4F). In agreement, Nestin (a hallmark of neuronal lineage

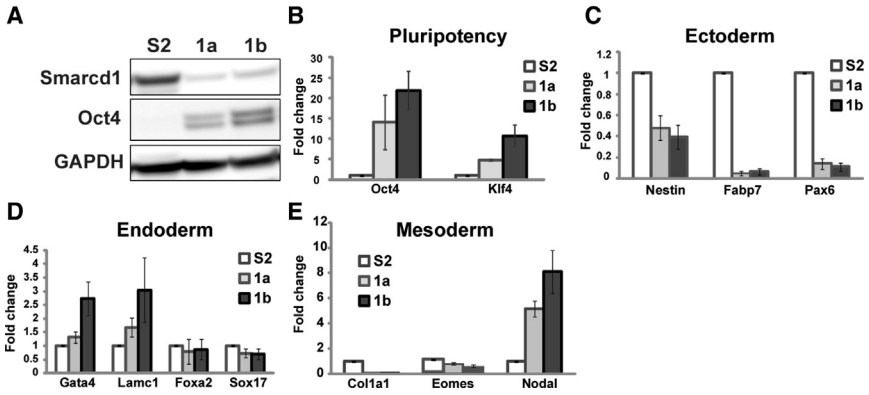

Figure 3. SMARCD1 Knockdown Leads to Improper Gene Expression in Embryoid Bodies

(A) WB of SMARCD1 and OCT4 in embryoid bodies from SMARCD1-KD clones and controls (representative pictures from two independent experiments are shown).

(B) qPCR analysis of pluripotency markers OCT4 and KLF4 in EBs from SMARCD1-KD clones and controls. The graph represents average gene expression levels from three independent biological repeats ± SEM normalized to the expression levels of LMNB2.

(C) Same as (B) for ectodermal markers NESTIN, FABP7, and PAX6.

(D) Same as (B) for endodermal markers GATA4, LAMC1, FOXA2, and SOX17.

(E) Same as (B) for mesodermal markers COL1a1, EOMES, and NODAL.

specification) levels, determined by WBs (Figure 4G) and qPCR (Figure 5H), were significantly reduced, and the number of Nestin-positive cells, determined by immunofluorescence staining (Figure 4H), decreased by over 2-fold in both fluorescence levels and the percentage of Nestin-positive cells (Figures 4I and 4J). Cell re-organization upon RA-induced differentiation was also affected by SMARCD1 KD. While control cells grew as a uniform monolayer, SMARCD1-KD cells organized into two distinct morphological populations that differed by the expression of Nestin or GATA4 (Figure 4I) in one sub-population and Lamininβ1 or FOXA2 in the other (Figures S4A and S4B). RA-induced, FOXA2-positive, SMARCD1-KD cells also showed elevated levels of KLF4 (Figure S4B) and directed endodermal differentiation (Christodoulou et al., 2011) resulted in enhanced endodermal marker expression in the SMARCD1-KD clones compared with WT (Figure S4C). We thus tested whether the increased KLF4 levels in these cells may explain the perturbed differentiation phenotypes by repeating these experiments under low-KLF4 conditions using infection with KLF4-specific shRNAs. When KLF4 was silenced in the differentiating SMARCD1-KD cells, the exaggerated endodermal differentiation phenotype was almost completely restored (Figure S4D), suggesting that the failure to silence KLF4 in the SMARCD1-KD cells is largely responsible for the perturbed differentiation phenotype. LacZ-KD, used as control, did not rescue these phenotypes (Figure S4D), and KD of KLF4 in control cells had no effect (Figure S4D, bottom). Taken together, these results demonstrate that SMARCD1 is essential for ESC differentiation and that its reduction leads to enhanced endodermal differentiation, mediated largely by the failure to repress KLF4, at the expense of ectodermal and mesodermal differentiation.

Gene Expression Analyses Support Differentiation Abnormalities

In order to understand global effects of SMARCD1 KD on gene expression and the role of SMARCD1 in proper ESC differentiation, we analyzed changes in gene expression in both undifferentiated ESCs and in RA-treated ESCs (4 days) (Table S4). The different SMARCD1-KD clones showed very good reproducibility and clustered together by Pearson's correlation (Figure 5A). To validate the microarray results, we performed qPCR for a variety of different genes in both ESCs and RA-induced differentiated cells and found a very high correlation between the microarray and qPCR results ($R^2 = 0.844$) (Figures 5B and 5E–5J).

Since the esBAF complex was shown to act as both an activator and a repressor (Ho et al., 2009a), we speculated that SMARCD1 KD would lead to both upregulation and downregulation of genes. Indeed, 236 genes were upregulated and 511 genes were downregulated in SMARCD1-KD ESCs. This trend was much more prominent in the RA-differentiated cells, with 1,088 upregulated and 1,240 downregulated genes (Figure 5C). Gene Ontology (GO) analysis for genes downregulated in RA-differentiating KD clones showed the most significant score ($p < 0.001$) and included terms related to differentiation and cellular regulation (Figure S5A), DNA binding (Figure S5B), and extracellular matrix (ECM) (Figure S5C), compared with control cells. A closer examination of the perturbed genes showed downregulation of ectodermal (e.g., Nes, Sema3a, and Vim) (Figure S5D) and mesodermal (e.g., Col1a1, Col2a1, and Wt1) (Figure S5E) markers and upregulation of endodermal markers (e.g., Gata4, Gata6, and Sox7) upon differentiation (Figure S5F). Pluripotency markers were upregulated both before and after differentiation (Figures 5D–5G). Overall, our gene expression analyses support the cellular phenotype we observed in relation to mesodermal and ectodermal differentiations and indicate that SMARCD1 is important for ESC differentiation, either directly or indirectly.

SMARCD1 Is Involved in Gene Regulation and Ectodermal Differentiation

Since SMARCD1 KD significantly affected gene expression, the next step in our inquiry was to identify its genomic targets. To this end, we performed chromatin immunoprecipitation (ChIP) followed by high-throughput sequencing (ChIP-seq) using SMARCD1-specific antibodies in both undifferentiated and RA-induced differentiated (4 days) ESCs. We found that SMARCD1 binding was significantly enriched in genic regions, where it predominantly bound exonic and intronic regions and, to a somewhat lesser extent, 3′ UTRs and promoter regions (Figure 6A). SMARCD1 was found to bind 2,112 genes in undifferentiated

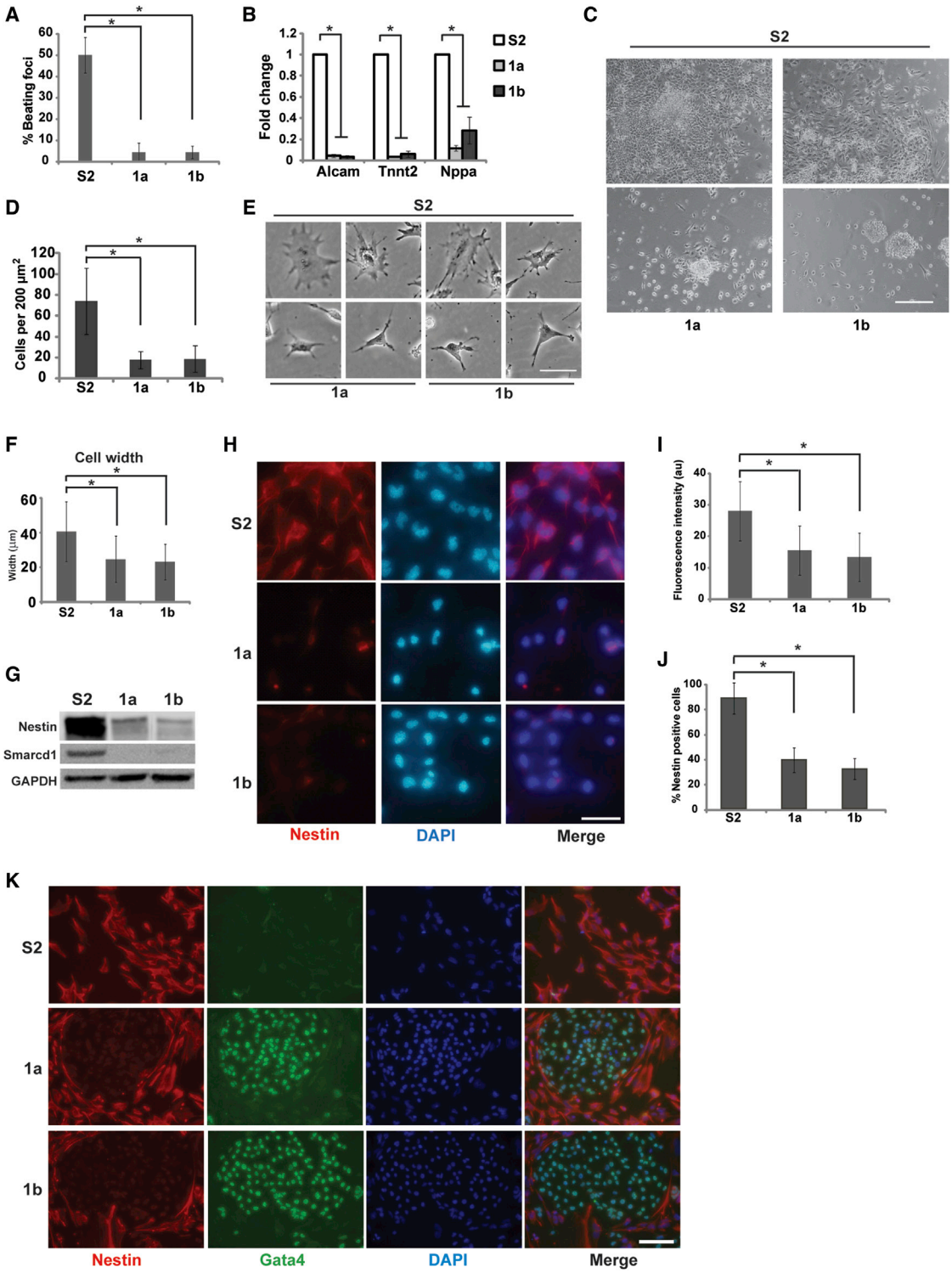

Figure 4. Impaired Differentiation in SMARCD1-Knockdown Clones

(A) Quantification of the number of beating foci in the SMARCD1-KD clones (1a and 1b) and controls (S2) after 10 days of cardiomyocyte differentiation. Shown are mean values of three independent experiments ± SEM. Changes are significant ($p < 0.01$; two-tailed Student's t test).

(B) qPCR analysis of cardiomyocyte markers ALCAM, TNNT2, and NPPA in SMARCD1-KD clones and controls. The graph represents average gene expression levels ± SEM normalized to the expression levels of GAPDH from three independent experiments. Changes are significant ($p < 0.0002$, two-tailed Student's t test).

(C) NPC formation in SMARCD1-KD clones (1a and 1b) and controls (S2). Scale bar, 200 µm.

(legend continued on next page)

cells and 2,406 genes in differentiated cells (Table S5). Comparing these two groups, we found that ~30% of the genes are bound by SMARCD1 both before and after 4 days of differentiation (Figure 6B; $p < 10^{-9}$, Fisher's exact test). GO analysis revealed that SMARCD1 binds genes that belong to two main "biological processes": "regulation" and "development." Interestingly, these two GO categories were dominant both before and after differentiation (Figures S6A and S6B), despite the fact that only ~30% of the genes are shared. Further examination of the three groups (genes specific to ESCs, shared genes, and genes specific to RA) using GO analysis revealed that the shared genes and genes specific to RA belong to the same biological processes: regulation and development. The main category of the ESCs specific genes was "cell cycle." Interestingly, regulation and development were also found to be the main categories that characterize the genes with altered expression in differentiating KD cells when compared with differentiated control cells (Figure S5A). Taken together, this strongly suggests a direct role for SMARCD1 in the regulation of genes involved in these two biological processes.

Peak distribution of SMARCD1 around the TSS (±5 kb) showed that SMARCD1 binds the promoter region, is depleted in the TSS, and binds again in the gene body with an even stronger signal (Figure 6C). This pattern is common to both pluripotent and RA-induced differentiating cells, although RA-treated cells show a more pronounced enrichment in gene bodies (Figure 6C, red). Interestingly, the distribution pattern of SMARCD1 around the TSS resembles that of H3K27me3 (Figure 7E). To further analyze the correlation between the binding pattern of SMARCD1 at genes and its effect on gene expression, we analyzed changes in gene expression in respect to SMARCD1 binding. We found that SMARCD1 was significantly enriched in genes that were downregulated upon KD: 81 out of 511 and 196 out of 1,125 genes were bound by SMARCD1 in ESCs and in RA-induced cells, respectively ($p = 0.00015$ in ESC and $p < 10^{-9}$ in RA, Fisher's exact test). In the upregulated genes (upon SMARCD1 KD), significance levels were marginal, with 36 out of 236 genes in ESCs ($p = 0.017$, Fisher's exact test) and 149 out of 1,084 in RA-treated samples ($p = 0.046$, Fisher's exact test). These data suggest that SMARCD1 is required for the induction of a core set of genes.

Because of the perturbed differentiation phenotype, we next analyzed the binding pattern of SMARCD1 to well-established 42 genes related to development and differentiation of the three germ layers (Table S2). While in endoderm and mesoderm no significant enrichment or correlation was found, we detected a significant enrichment of SMARCD1 binding in ectodermal genes after RA differentiation (Table S2). 5 of the 15 genes that were tested were bound by SMARCD1 ($p = 0.02$, Fisher's exact test), and remarkably, the expression level of all of these bound genes was reduced when SMARCD1 was knocked down (Table S2). Taken together, these results imply a direct positive regulation of ectodermal genes by SMARCD1 during RA-induced differentiation.

SMARCD1 Co-localizes with Pluripotency Master Regulators and p53

We next wished to correlate the binding profile of SMARCD1 with pluripotency factors. To this end, we analyzed previously published ChIP-seq datasets in correlation with our own. Since SMARCD1 is part of the esBAF complex, we first checked whether we could detect co-localization between SMARCD1 and BRG1, the catalytic subunit of the complex. As expected, we found a highly significant co-localization of the two proteins ($p < 10^{-9}$, Fisher's exact test). In addition, we found significant co-localization of SMARCD1 with several pluripotency master regulators including OCT4, NANOG, and SOX2, but not KLF4 ($p < 10^{-9}$, $p = 8 \times 10^{-5}$, $p = 0.0068$, and $p = 0.0745$, respectively, Fisher's exact test). Finally, we tested the potential co-association of SMARCD1 with proteins that were found to bind SMARCD1. A literature search revealed that TP53 (p53) (Oh et al., 2008) and SOX2 (Gao et al., 2012) associated directly with SMARCD1. We found that SMARCD1 co-localizes significantly with TP53 ($p = 4 \times 10^{-6}$, Fisher's exact test), but only with the activated, phosphorylated form of p53, p53S18. Significance levels were much more marginal for the unphosphorylated p53 ($p = 0.0022$, Fisher's exact test), likely due to the fact that the anti-p53 antibody recognizes both the unphosphorylated and the phosphorylated forms. Taken together, these data imply a potential role for SMARCD1 in regulating the expression of genes governed by pluripotency-related TFs and suggest that SMARCD1 associates with the active, but not the inactive, form of p53. The specific nature of this interaction remains to be defined.

SMARCD1 Is Associated with Bivalent Genes

Since many of the genes that were affected by SMARCD1 KD have a role in differentiation, and since SMARCD1 binding patterns resembled H3K27me3 binding patterns, we hypothesized that they might be marked with the "bivalent" histone modifications H3K4me3 and H3K27me3. Indeed, we detected a marked enrichment for bivalent genes bound by SMARCD1, especially in

(D) Quantification of the number of cells per 200 μm^2 ± SEM. Changes are significant ($p < 0.007$, two-tailed Student's t test).
(E) Cell morphology in SMARCD1 clones (lower panel) compared with S2 controls (upper panel) (scale bar, 50 μm) following RA-induced differentiation.
(F) Quantification of cell length ± SEM. Changes are significant ($n = 100$; $p < 10^{-10}$, two-tailed Student's t test).
(G) WB of SMARCD1-KD clones and controls shows reduction in SMARCD1 and NESTIN levels following SMARCD1 KD. GAPDH was used for normalization (representative pictures from two independent experiments are shown).
(H) Immunostaining of RA-induced SMARCD1-KD clones (1a and 1b) and S2 controls with anti-NESTIN antibodies (red, left panel). DAPI (blue), middle panel; right, merge. Scale bar, 50 μm.
(I) Quantification of (H). Graph represents NESTIN fluorescence intensity in RA-induced SMARCD1-KD clones (1a and 1b) and S2 controls.
(J) Quantification of (H) ± SEM. Graph represents the percentage of NESTIN positive cells in the RA-induced SMARCD1-KD clones (1a, 1b) versus controls ($p < 0.05$, two-tailed Student's t test). In (I) and (J), 80–150 cells were counted in each experiment.
(K) Co-immunostaining of RA-induced SMARCD1-KD clones (1a and 1b) and controls using anti-NESTIN (red) and anti-GATA4 (green) antibodies. DAPI (blue), middle panel; right, merge. Scale bar, 125 μm.

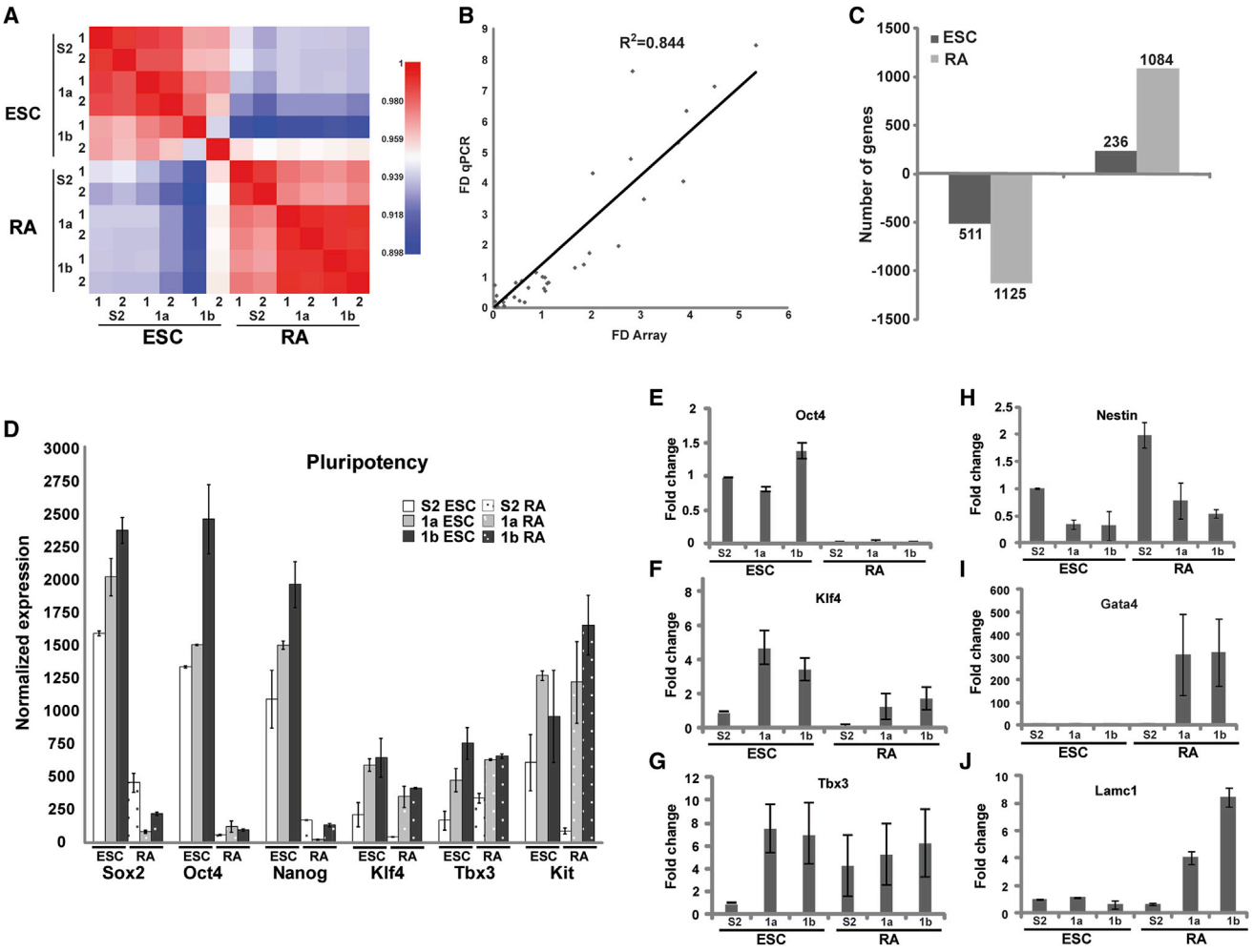

Figure 5. Aberrant Expression of Pluripotency and Lineage Markers in SMARCD1-KD Cells

(A) Expression analysis of SMARCD1-KD and control clones before and after RA differentiation. Pearson's correlation was used to calculate similarity. Red denotes $p > 0.95$; blue denotes $p < 0.95$. Numbers represent biological replicates.

(B) Microarray validation using real-time RT-PCR (qPCR). The expression level of seven genes in both ESC and RA groups was measured. GAPDH was used for normalization. Microarray and qPCR data are highly correlated ($R^2 = 0.84$).

(C) Quantification of up- and downregulated genes (>1.5-fold) in SMARCD1-KD and control clones in both ESC and RA-treated groups.

(D) Expression level (microarray) of pluripotency markers in ESC and RA-treated cells (shown are mean values ± SEM of two biological replicates).

(E–J) qPCR analysis of OCT4 (E), KLF4 (F), TBX3 (G), NESTIN (H), GATA4 (I), and LAMC1 (J) in ESC and RA-treated cells. Shown are mean values ± SEM of two biological replicates.

genes that were downregulated in the SMARCD1-KD cells (122 out of 511 in ESCs and 273 out of 1125 in RA-treated cells; $p < 10^{-9}$ in both groups, Fisher's exact test). Genes that were upregulated in the KD cells showed a more modest enrichment (44 out of 236 in ESCs and 173 out of 1084 in RA-treated cells; $p = 0.017$ and $p = 0.011$, respectively, Fisher's exact test). These results called for studying the genome-wide patterns of H3K4me3 and H3K27me3 in SMARCD1-KD clones.

SMARCD1 Regulates H3K4me3 and H3K27me3 Distribution

We next performed ChIP-seq for H3K4me3 and H3K27me3 in SMARCD1-KD and control cells. Analyzing H3K4me3/H3K27me3 global distributions showed that both modifications exhibited altered levels in the SMARCD1-KD cells, both before and after RA-induced differentiation. 13,024 genes were marked with H3K4me3 in both control and KD cells, 1,004 genes were marked with H3K4me3 in control cells only, and 2,224 genes were marked with H3K4me3 in KD cells only (Figure 7A). Hence, the number of genes marked with H3K4me3 was slightly elevated in the KD cells. After differentiation, the number of genes marked with H3K4me3 in KD cells was considerably elevated. 13,676 genes were marked with H3K4me3, 46 genes were marked with H3K4me3 in control cells, and 2,952 genes were marked with H3K4me3 in KD cells (Figure 7A). Western blot analysis showed no discernible change in the global levels of H3K4me3 in the KD cells compared to the control cells both before and after differentiation (Figure S7A).

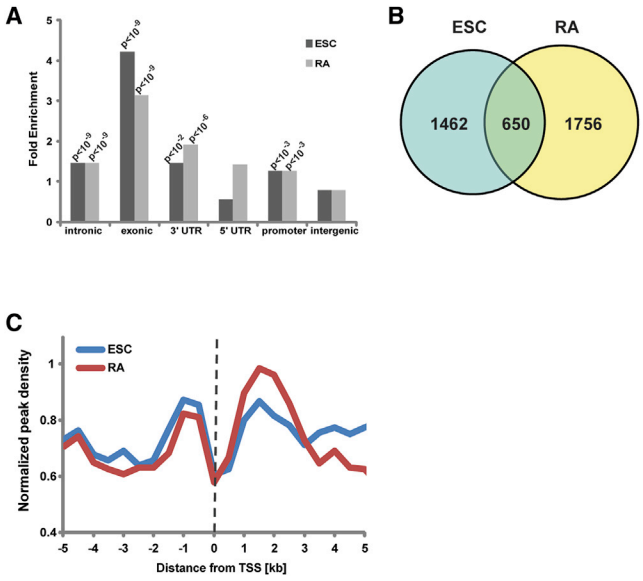

Figure 6. SMARCD1 Is Enriched in Genic Regions

(A) SMARCD1 binding sites enrichment in intergenic and genic regions (5′ UTR, 3′ UTR, exonic, promoter, and intronic) in ESCs (dark gray) and in RA-induced cells (RA, light gray). Note highly significant enrichment in intronic and exonic regions and significant enrichment in promoter and 3′ UTR regions.

(B) Venn diagram of genes bound by SMARCD1 from ESCs (left) and RA-induced differentiated cells (right). 650 genes overlap, 1,462 are unique for ESCs, and 1,756 are unique for RA-induced differentiated cells ($p < 10^{-9}$, Fisher's exact test).

(C) SMARCD1 distribution ±5 kb around the transcription start site (TSS) in ESCs (blue) and in RA-induced cells (RA, red).

Interestingly, unlike H3K4me3, which showed the same trend in pluripotent and differentiating ESCs, the number of genes marked with H3K27me3 exhibited an opposite trend; in undifferentiated ESCs, 3,304 genes were marked with H3K27me3 in both control and KD cells, 239 genes were marked with H3K27me3 in control cells only, and 2,413 genes were marked with H3K27me3 in KD cells only. Hence, the number of genes marked with H3K27me3 was considerably elevated in the KD cells. Upon differentiation, the number of genes marked with H3K27me3 in the KD cells was dramatically reduced by 78%; 582 genes were marked with H3K27me3 in both groups, 2,826 genes were marked with H3K27me3 in control cells only, and 155 genes were marked with H3K27me3 in KD cells only (Figure 7B). Surprisingly, quantification of H3K27me3 levels by western blotting of isolated chromatin fractions in SMARCD1-KD versus control cells showed a slight increase in H3K27me3 level in the SMARCD1-KD cells, both in undifferentiated and in differentiated cells (Figure S7B), suggesting that it is not the total H3K27me3 chromatin bound fraction that was altered upon SMARCD1-KD but rather its distribution, with a selective decrease in genic regions.

We therefore tested the levels of H3K4me3 and H3K27me3 around genic regions, ±5 kb from the TSS. In ESCs, the characteristic H3K4me3 distribution around the TSS was overall preserved in SMARCD1-KD cells, albeit with a small elevation just before the TSS (Figure 7C). This elevation was more pronounced in RA-induced differentiating SMARCD1-KD cells (Figure 7D). The opposite phenomenon was observed for H3K27me3 patterns: a slight reduction in H3K27me3 around the TSS was observed in undifferentiated SMARCD1-KD ESCs (Figure 7E), which was almost completely abolished in RA-treated cells (Figure 7F).

SMARCD1 Binding Is Associated with Gene Induction during Differentiation

To ask whether up- or downregulated genes upon SMARCD1 KD are differentially marked by H3K4me3 and H3K27me3 levels, we compared H3K4me3 and H3K27me3 ChIP-seq data with the SMARCD1-KD gene expression data. The read density spanning ±5 kb of TSSs of 19,885 genes from the RefSeq database was compared with genes that were sorted according to the expression array: from genes that were highly expressed in the KD clones to genes that were highly expressed in the control cells. A general elevation of both H3K4me3 and H3K27me3 at genic regions can be seen in undifferentiated SMARCD1-KD ESCs, regardless of the expression level of the bound genes (Figure 7G). However, within the over 500 downregulated genes, the ~25% most significantly downregulated displayed markedly reduced H3K4me3 levels (Figure 7G, bottom left), potentially explaining their downregulation. Also, in this group of genes, the elevation of H3K27me3 was most pronounced (Figure 7G, bottom right). In the RA-differentiated cells, H3K4me3 levels were elevated across the upregulated genes and unaltered across the downregulated genes in the SMARCD1-KD clones (Figure 7H, left). In stark contrast, H3K27me3 levels were dramatically decreased in the SMARCD1-KD cells across all the genes regardless of their expression level (Figure 7H, right), although this decrease was most significant in the upregulated genes. Taken together, these data suggest that SMARCD1 regulates genic distribution of H3K4me3 and mostly of H3K27me3, regulating, at least to some extent, the expression of these genes.

SMARCD1 Regulates KLF4 in a Direct and Indirect Manner

As noted earlier, a key TF that had higher expression levels in both ESCs and RA-treated cells following SMARCD1 KD is KLF4 (Figures 5D and 5F). To test whether the expression of KLF4 can be explained by H3K4me3/H3K27me3 levels, we examined both these marks around *Klf4*'s TSS and in the gene body itself (Figure 7I). In the undifferentiated state, H3K4me3 levels were higher in the KD cells compared with the control cells, while H3K27me3 levels were low in both KD and control cells. This may explain the high levels of KLF4 in both KD clones 1a and 1b (~4.8- and ~3.5-fold, respectively) (Figure 5F). Following RA-induced differentiation, H3K4me3, but not H3K27me3, showed a similar trend to the one observed in the ESC state. H3K4me3 levels were higher in the KD clones compared to the control cells and H3K27me3 was almost abolished in the KD clones, again probably explaining the high levels of KLF4 in both KD clones (~7- and ~9.7-fold, respectively) (Figure 5F). In addition, SMARCD1 was found to be associated with *Klf4*'s promoter, 4 kb upstream of the TSS, in undifferentiated, but not differentiated, ESCs (Figure 7I, red box), suggesting a direct association of SMARCD1 with the *Klf4* gene. To test if

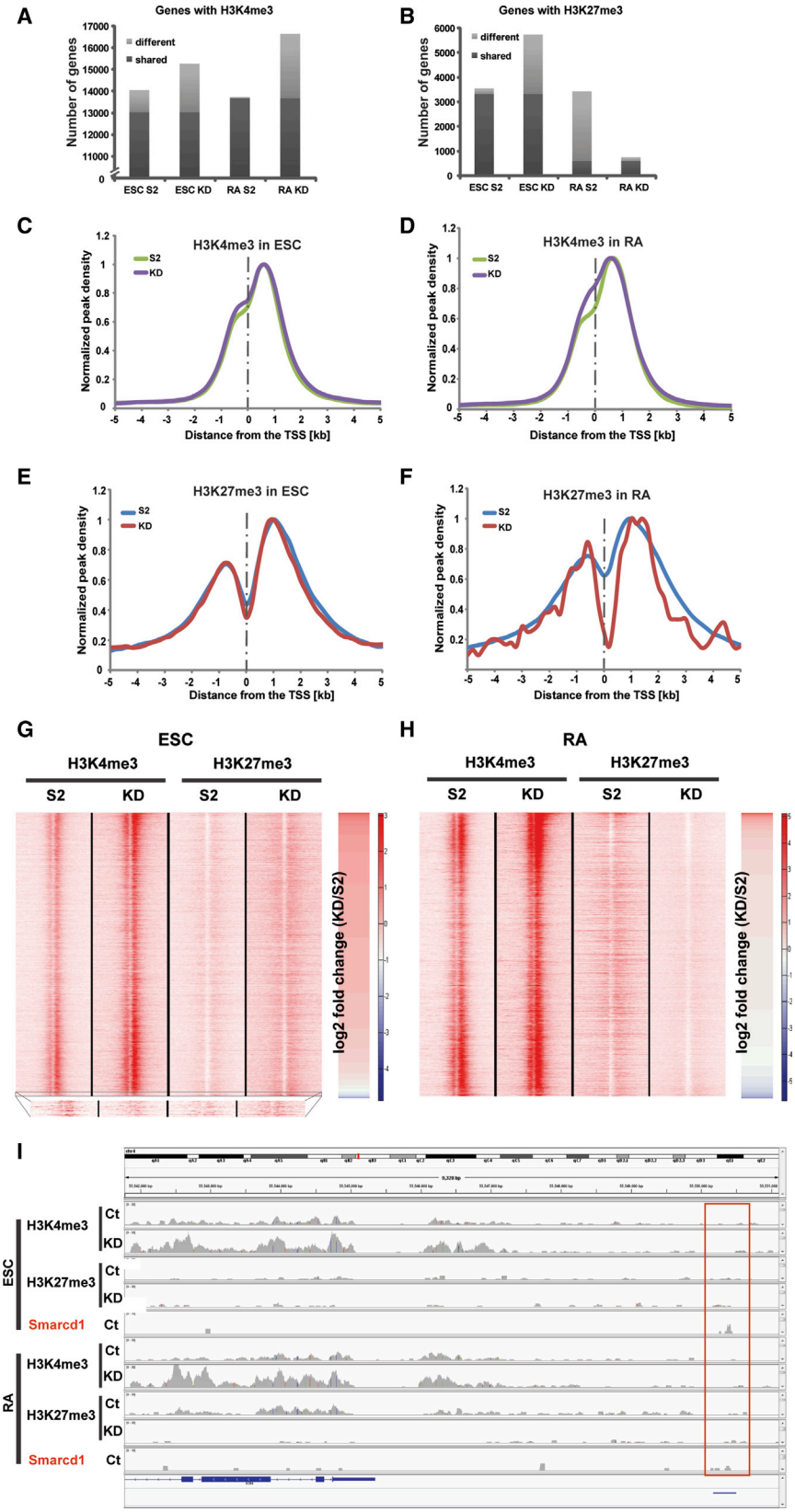

Figure 7. SMARCD1 Controls H3K4me3 and H3K27me3 Distribution around TSSs

(A) The number of genes enriched with H3K4me3 in ESCs and in RA-induced cells. Shared genes are labeled with dark gray.

(B) The number of genes enriched with H3K27me3 in ESCs and in RA-induced cells. Shared genes are labeled with dark gray. Note the reduction in the number of H3K27me3 marked genes in the RA-induced KD cells.

(C and D) Composite plot of normalized H3K4me3 peaks ±5 kb around the TSS in KD (purple) and S2 control (green) ESC (C) and RA-induced (D) clones.

(E and F) Same as (C) and (D) for H3K27me3.

(G) Read densities of H3K4me3 and H3K27me3 in ESC in a window of 10 kb around the TSSs of 19,885 RefSeq genes. Genes were sorted from highly expressed in the KD clones to highly expressed in control cells based on the expression arrays.

(H) Same as (G) for RA-differentiated clones.

(I) H3K4me3, H3K27me3, and SMARCD1 read density around *Klf4*'s promoter, TSS, and gene body in ESCs (top) and RA-induced cells (RA) (bottom). Red box denotes a MACS peak of SMARCD1 in undifferentiated ESCs 4 kb upstream of Klf4's promoter. The Klf4 gene (bottom) is shown in blue, from right to left.

depletion of SMARCD1 results in clearance of the *Klf4* promoter from other esBAF components, we performed ChIP-qPCR for BRG1 and found a slight but consistent enrichment (2-fold) on the *Klf4* promoter (Figure S7C). The *Oct4* promoter showed no such enrichment (Figure S7C). Taken together, these data suggest that SMARCD1 acts to silence KLF4 by regulating the levels of H3K27me3 at the *Klf4* promoter. Its co-expression with the endodermal marker FOXA2 in the RA-differentiated SMARCD1-KD cells, as well as a recent report that suggested its role in early endodermal differentiation (Cao et al., 2012), may explain the preferred endodermal over ectodermal differentiation observed in the SMARCD1-KD cells.

DISCUSSION

In this study, we present a useful biochemical assay, D-CAP, for the identification of proteins that are differentially bound to chromatin between two cell types. We employed this assay to characterize and compare the differential association of proteins to chromatin in pluripotent ESCs and differentiating NPCs. Many of the proteins that we found to be associated with chromatin in ESCs are known to have an ESC-related role, e.g., HDAC1 (Dovey et al., 2010; Jurkin et al., 2011; Kidder and Palmer, 2012); DDX18, SNRPD2, and SMC1a (Fazzio et al., 2008); and SMARCC1 (Fazzio et al., 2008; Ho et al., 2009b; Schaniel et al., 2009). These published works, combined with our D-CAP results, suggest that chromatin-associated proteins have a functional role in ESC biology. D-CAP can be employed in ESCs to study various differentiation pathways but can also be harnessed to compare essentially any two or more cell types, including during development, in disease states, and following various treatments.

Unlike proteome analysis of whole-extract samples from nuclei of ESCs and differentiated cells (Barthélery et al., 2009; Kurisaki et al., 2005; Lu et al., 2009), D-CAP enables one to distinguish between proteins that are expressed roughly at similar levels but display differential association to chromatin, as we observed for SMARCC1 and SMARCD1. Although their protein levels in ESCs and NPCs remained unaltered, the association of these proteins with chromatin changed, possibly suggesting a different role for these as well as other proteins in ESCs and during differentiation. This was further verified by ChIP-seq, where only 30% of the genes (650/2,112) bound by SMARCD1 were common to both ESCs and RA-induced differentiating cells.

In contrast to other subunits of the esBAF complex (Gaspar-Maia et al., 2011; Ho et al., 2009b), in our hands, depletion of SMARCD1 had a limited effect on the pluripotent state of ESCs using both knockout and KD approaches. A recent study showed that in D3 ESCs, SMARCD1 KD led to spontaneous differentiation (Gao et al., 2012). This could be explained by different SMARCD1 levels achieved in different clones, leading to different esBAF subunit stoichiometry. Regardless, SMARCD1 KD in differentiating cells resulted in a much more prominent phenotype including aberrant differentiation and increased levels of pluripotency markers. Although complete KO of SMARCD1 did not affect undifferentiated ESCs, it resulted in extensive cell death when the cells were induced to differentiate. This suggests that SMARCD1 may act as a regulator of the pluripotency network, shutting down key components during the early stages of differentiation to enable differentiation to proceed. The only major difference observed in the undifferentiated state due to SMARCD1 KD was a more open chromatin conformation: HP1α distribution was affected, H3 acetylation levels were higher, and FRAP analysis revealed higher mobility of H1, which coincides with higher histone acetylation levels and a more relaxed chromatin state (Melcer et al., 2012). Increased histone acetylation and chromatin plasticity in ESCs was previously shown to have limited effect on the undifferentiated state (Boudadi et al., 2013; Hezroni et al., 2011b), in agreement with our current results.

While induction of NPCs and cardiomyocytes from SMARCD1-KD clones led to impaired differentiation, RA, which is a less selective differentiation agent, led to the generation of two distinct cell populations, each expressing a different lineage marker (NES or GATA4). This indicates that under these conditions, SMARCD1 KD led to a shift from ectodermal to endodermal differentiation. Our gene expression data, which showed upregulation of endodermal genes and downregulation of ectodermal genes in the RA-induced KD cells, strengthened this conclusion. It would be interesting to check whether SMARCD1-KD ESCs can differentiate more easily into endoderm and perhaps become a better source for endodermal differentiation, as our data suggest.

Our combined ChIP-seq and expression analyses suggest that SMARCD1 may regulate gene expression both directly and indirectly, likely through interactions with different TFs and transcriptional regulator complexes. Our ChIP-seq results suggest that TP53 (p53) is one of these SMARCD1 partners. SMARCD1 and p53 show a significantly high degree of co-localization, and p53 itself interacts with the SWI/SNF complex via SMARCD1 (Oh et al., 2008). In ESCs, p53 is important for the repression of key transcriptional regulators such as OCT4, NANOG, and SOX2 (Li et al., 2012). As indicated above, SMARCD1 is probably required to enable the repression of these TFs during early differentiation. In the absence of SMARCD1, the pluripotency factors escape repression, their expression remains high, and differentiation is severely inhibited.

Interestingly, SMARCD1 KD in ESCs had an opposite effect to a KD of another chromatin remodeler, CHD1, we previously studied (Gaspar-Maia et al., 2009). In both cases, the KD did not affect pluripotent marker expression in the undifferentiated state, but in contrast to SMARCD1, the CHD1-KD cells accumulated high levels of heterochromatin and differentiated precociously, suggesting that CHD1 acts to keep chromatin open, while SMARCD1 acts to keep chromatin closed. Regardless, both chromatin remodelers are important to establish the correct balance between euchromatin and heterochromatin in ESCs, which is likely critical for the maintenance of pluripotency.

How does SMARCD1 exert its effect on ESCs? Our combined ChIP-seq and gene expression studies suggest a two-level mechanism: first, by directly regulating the pluripotency-related factor KLF4, which is one of the four "Yamanaka factors" used for reprogramming somatic cells into induced pluripotent stem cells (iPSCs); and second, by a more global influence on chromatin structure by regulating the levels of histone modifications,

mostly of H3K27me3, which is required to silence developmental genes in ESCs, as well as pluripotency genes in differentiating cells (Bernstein et al., 2006; Mikkelsen et al., 2007; Pan et al., 2007; Zhao et al., 2007). This dual action is likely also mediated by other members of the esBAF complex of which SMARCD1 is a member. Depletion of SMARCD1 likely results in altered stoichiometry of the different subunits in the complex, potentially leading to its aberrant functioning. This is supported by more recent observations showing that depletion of the catalytic subunit of the esBAF complex, BRG1, also causes global changes in PRC2 and H3K27me3 (Ho et al., 2011).

To summarize, in this study, we present a method to identify chromatin-associated proteins that are enriched in one cell population over the other, and we employed it to identify differentially bound chromatin proteins between undifferentiated and partially differentiated ESCs. Using this method, which we named D-CAP, we identified the chromatin remodeling protein SMARCD1, which displayed more significant association with chromatin in ESCs compared to differentiated cells. Our functional studies suggest an important role for SMARCD1 in early differentiation events and for maintaining the balance between euchromatin and heterochromatin. In conclusion, our results demonstrate the role of SMARCD1 in restricting the pluripotency network and activating various differentiation pathways.

EXPERIMENTAL PROCEDURES

Cell Culture

Mouse R1 ESCs were cultured as described before (Melcer et al., 2012). Differentiation procedures are described in Supplemental Experimental Procedures.

Micrococcal Nuclease Digestion

Fresh nuclei from ESCs or NPCs were washed (four times), resuspended in MNase digestion buffer (10 mM Tris-HCl [pH 8], 5 mM $CaCl_2$, 150 mM KCl, 0.1 mM PMSF, and protease inhibitor cocktail 1:100 [Sigma]), rotated (4°C, 30 min), and centrifuged (500 × *g*, 4°C, 5 min). Nuclei were then subjected to different MNase concentrations (0/1.5/3/4.5/1,000 U/ml MNase [Worthington]) in MNase digestion buffer. Reactions were stopped by adding 10× MNase Stop Buffer (100 mM Tris-HCl [pH 7.5], 100 mM EDTA, and 10 mM EGTA) followed by centrifugation (13,000 × *g*, 4°C, 10 min). Supernatants were collected and subjected to LC-MS/MS analyses. To verify the MNase digestion, DNA was purified from the pellets and electrophoresed.

Gene Expression Analysis

Total RNA was extracted and subjected to GeneChip Mouse Gene 1.0ST Arrays (Affymetrix). Data were normalized with the robust multiarray average method using the Affymetrix Expression Console (version 1.1). See also Supplemental Experimental Procedures.

ChIP

ChIP was performed as described previously (Sailaja et al., 2012). Antibodies used included BRG1 (ab110641, Abcam), H3K4me3 (ab8580, Abcam), H3K27me3 (07-449, Millipore), and SMARCD1 (611728, BD). ChIP-seq was done as described previously (Hezroni et al., 2011a) using the SOLiD4 sequencer (ABI).

Mass Spectrometry of Proteins

Proteins were reduced, alkylated, and trypsinized as described previously (Dutta et al., 2012; Sanders et al., 2002). The peptides were subjected to reverse-phase microcapillary electrospray ionization LC-MS/MS. See also Supplemental Experimental Procedures.

ACCESSION NUMBERS

The GEO accession number for the expression data reported in this paper is GSE65089. SOLiD ChIP-seq data can be downloaded directly from the following website: http://meshorerlab.huji.ac.il/downloads.html.

SUPPLEMENTAL INFORMATION

Supplemental Information includes Supplemental Experimental Procedures, seven figures, and five tables and can be found with this article online at http://dx.doi.org/10.1016/j.celrep.2015.02.064.

AUTHOR CONTRIBUTIONS

A.A. designed and carried out all experiments following consultations with E.M.; A.B. performed ChIP-seq experiments and analyzed all ChIP-seq data; A.H. generated and validated the CRISPR-KO clones; B.S.S. performed ChIP experiments; Y.A. and I.L. helped with statistics and data analysis; M.N. helped with ChIP and IF experiments; A.G.S. and G.M. performed endodermal differentiation; and V.R.G., D.E.G., A.D., and S.K.S. performed LC-MS/MS experiments. A.A. and E.M. wrote the manuscript, and A.A., E.M., I.L., and A.B. discussed the results and commented on the manuscript.

ACKNOWLEDGMENTS

We thank Amichay Afriat and Tal Cohen for help with experiments, Shai Melcer for helpful discussions, and Abed A. Mansour and Jacob Hanna for kindly providing reagents. Microarray hybridization and high-throughput sequencing was carried out at The Center for Genomic Technologies, Institute of Life Sciences, The Hebrew University. This work was supported by the Israel Science Foundation (ISF 1252/12 and 657/12 to E.M.); the Israel Ministry of Science (E.M.), and the European Research Council (ERC-281781 to E.M.). A.B. is a Clore Fellow.

Received: July 21, 2014
Revised: January 9, 2015
Accepted: February 25, 2015
Published: March 26, 2015

REFERENCES

Barthéléry, M., Jaishankar, A., Salli, U., Freeman, W.M., and Vrana, K.E. (2009). 2-D DIGE identification of differentially expressed heterogeneous nuclear ribonucleoproteins and transcription factors during neural differentiation of human embryonic stem cells. Proteomics Clin. Appl. *3*, 505–514.

Bernstein, B.E., Mikkelsen, T.S., Xie, X., Kamal, M., Huebert, D.J., Cuff, J., Fry, B., Meissner, A., Wernig, M., Plath, K., et al. (2006). A bivalent chromatin structure marks key developmental genes in embryonic stem cells. Cell *125*, 315–326.

Bošković, A., Eid, A., Pontabry, J., Ishiuchi, T., Spiegelhalter, C., Raghu Ram, E.V., Meshorer, E., and Torres-Padilla, M.E. (2014). Higher chromatin mobility supports totipotency and precedes pluripotency in vivo. Genes Dev. *28*, 1042–1047.

Boudadi, E., Stower, H., Halsall, J.A., Rutledge, C.E., Leeb, M., Wutz, A., O'Neill, L.P., Nightingale, K.P., and Turner, B.M. (2013). The histone deacetylase inhibitor sodium valproate causes limited transcriptional change in mouse embryonic stem cells but selectively overrides Polycomb-mediated Hoxb silencing. Epigenetics Chromatin *6*, 11.

Boyer, L.A., Lee, T.I., Cole, M.F., Johnstone, S.E., Levine, S.S., Zucker, J.P., Guenther, M.G., Kumar, R.M., Murray, H.L., Jenner, R.G., et al. (2005). Core transcriptional regulatory circuitry in human embryonic stem cells. Cell *122*, 947–956.

Cao, Q., Zhang, X., Lu, L., Yang, L., Gao, J., Gao, Y., Ma, H., and Cao, Y. (2012). Klf4 is required for germ-layer differentiation and body axis patterning during Xenopus embryogenesis. Development *139*, 3950–3961.

Chen, X., Xu, H., Yuan, P., Fang, F., Huss, M., Vega, V.B., Wong, E., Orlov, Y.L., Zhang, W., Jiang, J., et al. (2008). Integration of external signaling pathways with the core transcriptional network in embryonic stem cells. Cell *133*, 1106–1117.

Chen, L., Fulcoli, F.G., Ferrentino, R., Martucciello, S., Illingworth, E.A., and Baldini, A. (2012). Transcriptional control in cardiac progenitors: Tbx1 interacts with the BAF chromatin remodeling complex and regulates Wnt5a. PLoS Genet. *8*, e1002571.

Christodoulou, C., Longmire, T.A., Shen, S.S., Bourdon, A., Sommer, C.A., Gadue, P., Spira, A., Gouon-Evans, V., Murphy, G.J., Mostoslavsky, G., and Kotton, D.N. (2011). Mouse ES and iPS cells can form similar definitive endoderm despite differences in imprinted genes. J. Clin. Invest. *121*, 2313–2325.

Dovey, O.M., Foster, C.T., and Cowley, S.M. (2010). Histone deacetylase 1 (HDAC1), but not HDAC2, controls embryonic stem cell differentiation. Proc. Natl. Acad. Sci. USA *107*, 8242–8247.

Dutta, B., Adav, S.S., Koh, C.G., Lim, S.K., Meshorer, E., and Sze, S.K. (2012). Elucidating the temporal dynamics of chromatin-associated protein release upon DNA digestion by quantitative proteomic approach. J. Proteomics *75*, 5493–5506.

Efroni, S., Duttagupta, R., Cheng, J., Dehghani, H., Hoeppner, D.J., Dash, C., Bazett-Jones, D.P., Le Grice, S., McKay, R.D., Buetow, K.H., et al. (2008). Global transcription in pluripotent embryonic stem cells. Cell Stem Cell *2*, 437–447.

Farthing, C.R., Ficz, G., Ng, R.K., Chan, C.-F., Andrews, S., Dean, W., Hemberger, M., and Reik, W. (2008). Global mapping of DNA methylation in mouse promoters reveals epigenetic reprogramming of pluripotency genes. PLoS Genet. *4*, e1000116.

Fazzio, T.G., Huff, J.T., and Panning, B. (2008). An RNAi screen of chromatin proteins identifies Tip60-p400 as a regulator of embryonic stem cell identity. Cell *134*, 162–174.

Gao, Z., Cox, J.L., Gilmore, J.M., Ormsbee, B.D., Mallanna, S.K., Washburn, M.P., and Rizzino, A. (2012). Determination of protein interactome of transcription factor Sox2 in embryonic stem cells engineered for inducible expression of four reprogramming factors. J. Biol. Chem. *287*, 11384–11397.

Gaspar-Maia, A., Alajem, A., Polesso, F., Sridharan, R., Mason, M.J., Heidersbach, A., Ramalho-Santos, J., McManus, M.T., Plath, K., Meshorer, E., and Ramalho-Santos, M. (2009). Chd1 regulates open chromatin and pluripotency of embryonic stem cells. Nature *460*, 863–868.

Gaspar-Maia, A., Alajem, A., Meshorer, E., and Ramalho-Santos, M. (2011). Open chromatin in pluripotency and reprogramming. Nat. Rev. Mol. Cell Biol. *12*, 36–47.

Hezroni, H., Sailaja, B.S., and Meshorer, E. (2011a). Pluripotency-related, valproic acid (VPA)-induced genome-wide histone H3 lysine 9 (H3K9) acetylation patterns in embryonic stem cells. J. Biol. Chem. *286*, 35977–35988.

Hezroni, H., Tzchori, I., Davidi, A., Mattout, A., Biran, A., Nissim-Rafinia, M., Westphal, H., and Meshorer, E. (2011b). H3K9 histone acetylation predicts pluripotency and reprogramming capacity of ES cells. Nucleus *2*, 300–309.

Ho, L., Jothi, R., Ronan, J.L., Cui, K., Zhao, K., and Crabtree, G.R. (2009a). An embryonic stem cell chromatin remodeling complex, esBAF, is an essential component of the core pluripotency transcriptional network. Proc. Natl. Acad. Sci. USA *106*, 5187–5191.

Ho, L., Ronan, J.L., Wu, J., Staahl, B.T., Chen, L., Kuo, A., Lessard, J., Nesvizhskii, A.I., Ranish, J., and Crabtree, G.R. (2009b). An embryonic stem cell chromatin remodeling complex, esBAF, is essential for embryonic stem cell self-renewal and pluripotency. Proc. Natl. Acad. Sci. USA *106*, 5181–5186.

Ho, L., Miller, E.L., Ronan, J.L., Ho, W.Q., Jothi, R., and Crabtree, G.R. (2011). esBAF facilitates pluripotency by conditioning the genome for LIF/STAT3 signalling and by regulating polycomb function. Nat. Cell Biol. *13*, 903–913.

Hsiao, P.W., Fryer, C.J., Trotter, K.W., Wang, W., and Archer, T.K. (2003). BAF60a mediates critical interactions between nuclear receptors and the BRG1 chromatin-remodeling complex for transactivation. Mol. Cell. Biol. *23*, 6210–6220.

Jurkin, J., Zupkovitz, G., Lagger, S., Grausenburger, R., Hagelkruys, A., Kenner, L., and Seiser, C. (2011). Distinct and redundant functions of histone deacetylases HDAC1 and HDAC2 in proliferation and tumorigenesis. Cell Cycle *10*, 406–412.

Kidder, B.L., and Palmer, S. (2012). HDAC1 regulates pluripotency and lineage specific transcriptional networks in embryonic and trophoblast stem cells. Nucleic Acids Res. *40*, 2925–2939.

Kidder, B.L., Palmer, S., and Knott, J.G. (2009). SWI/SNF-Brg1 regulates self-renewal and occupies core pluripotency-related genes in embryonic stem cells. Stem Cells *27*, 317–328.

Kurisaki, A., Hamazaki, T.S., Okabayashi, K., Iida, T., Nishine, T., Chonan, R., Kido, H., Tsunasawa, S., Nishimura, O., Asashima, M., and Sugino, H. (2005). Chromatin-related proteins in pluripotent mouse embryonic stem cells are downregulated after removal of leukemia inhibitory factor. Biochem. Biophys. Res. Commun. *335*, 667–675.

Lessard, J.A., and Crabtree, G.R. (2010). Chromatin regulatory mechanisms in pluripotency. Annu. Rev. Cell Dev. Biol. *26*, 503–532.

Li, M., He, Y., Dubois, W., Wu, X., Shi, J., and Huang, J. (2012). Distinct regulatory mechanisms and functions for p53-activated and p53-repressed DNA damage response genes in embryonic stem cells. Mol. Cell *46*, 30–42.

Lu, R., Markowetz, F., Unwin, R.D., Leek, J.T., Airoldi, E.M., MacArthur, B.D., Lachmann, A., Rozov, R., Ma'ayan, A., Boyer, L.A., et al. (2009). Systems-level dynamic analyses of fate change in murine embryonic stem cells. Nature *462*, 358–362.

Melcer, S., Hezroni, H., Rand, E., Nissim-Rafinia, M., Skoultchi, A., Stewart, C.L., Bustin, M., and Meshorer, E. (2012). Histone modifications and lamin A regulate chromatin protein dynamics in early embryonic stem cell differentiation. Nat. Commun. *3*, 910.

Meshorer, E., Yellajoshula, D., George, E., Scambler, P.J., Brown, D.T., and Misteli, T. (2006). Hyperdynamic plasticity of chromatin proteins in pluripotent embryonic stem cells. Dev. Cell *10*, 105–116.

Mikkelsen, T.S., Ku, M., Jaffe, D.B., Issac, B., Lieberman, E., Giannoukos, G., Alvarez, P., Brockman, W., Kim, T.K., Koche, R.P., et al. (2007). Genome-wide maps of chromatin state in pluripotent and lineage-committed cells. Nature *448*, 553–560.

Oh, J., Sohn, D.H., Ko, M., Chung, H., Jeon, S.H., and Seong, R.H. (2008). BAF60a interacts with p53 to recruit the SWI/SNF complex. J. Biol. Chem. *283*, 11924–11934.

Pan, G., Tian, S., Nie, J., Yang, C., Ruotti, V., Wei, H., Jonsdottir, G.A., Stewart, R., and Thomson, J.A. (2007). Whole-genome analysis of histone H3 lysine 4 and lysine 27 methylation in human embryonic stem cells. Cell Stem Cell *1*, 299–312.

Sailaja, B.S., Takizawa, T., and Meshorer, E. (2012). Chromatin immunoprecipitation in mouse hippocampal cells and tissues. Methods Mol. Biol. *809*, 353–364.

Sanders, S.L., Jennings, J., Canutescu, A., Link, A.J., and Weil, P.A. (2002). Proteomics of the eukaryotic transcription machinery: identification of proteins associated with components of yeast TFIID by multidimensional mass spectrometry. Mol. Cell. Biol. *22*, 4723–4738.

Schaniel, C., Ang, Y.S., Ratnakumar, K., Cormier, C., James, T., Bernstein, E., Lemischka, I.R., and Paddison, P.J. (2009). Smarcc1/Baf155 couples self-renewal gene repression with changes in chromatin structure in mouse embryonic stem cells. Stem Cells *27*, 2979–2991.

Serrano, L., Vazquez, B.N., and Tischfield, J. (2013). Chromatin structure, pluripotency and differentiation. Exp. Biol. Med. (Maywood) *238*, 259–270.

Skottman, H., Mikkola, M., Lundin, K., Olsson, C., Strömberg, A.M., Tuuri, T., Otonkoski, T., Hovatta, O., and Lahesmaa, R. (2005). Gene expression signatures of seven individual human embryonic stem cell lines. Stem Cells *23*, 1343–1356.

Zhao, X.D., Han, X., Chew, J.L., Liu, J., Chiu, K.P., Choo, A., Orlov, Y.L., Sung, W.K., Shahab, A., Kuznetsov, V.A., et al. (2007). Whole-genome mapping of histone H3 Lys4 and 27 trimethylations reveals distinct genomic compartments in human embryonic stem cells. Cell Stem Cell *1*, 286–298.